A mutation in the first intracellular loop of CACNA1A prevents P/Q channel modulation by SNARE proteins and lowers exocytosis

Selma A. Serra[a], Ester Cuenca-León[b], Artur Llobet[c], Francisca Rubio-Moscardo[a], Cristina Plata[a], Oriel Carreño[d], Noèlia Fernàndez-Castillo[d], Roser Corominas[b,d], Miguel A. Valverde[a], Alfons Macaya[b], Bru Cormand[d], and José M. Fernández-Fernández[a,1]

[a]Laboratory of Molecular Physiology and Channelopathies, Department of Experimental and Health Sciences, Universitat Pompeu Fabra, 08003 Barcelona, Spain; [b]Grup de Recerca en Neurologia Infantil, Hospital Universitari Vall d'Hebron, 08035 Barcelona, Spain; [c]Laboratori de Neurobiologia, Bellvitge Institute for Biomedical Research (IDIBELL)-Centro de Investigación Biomédica en Red Enfermedades Neurodegenerativas (CIBERNED), L'Hospitalet de Llobregat, 08907 Barcelona, Spain; and [d]Departament de Genètica, Universitat de Barcelona, Centro de Investigación Biomédica en Red de Enfermedades Raras, Institut de Biomedicina de la Universitat de Barcelona, 08028 Barcelona, Spain

Edited by Ramón Latorre, Centro de Neurociencias, Universidad de Valparaíso, Valparaíso, Chile, and approved December 11, 2009 (received for review July 24, 2009)

Familial hemiplegic migraine (FHM)-causing mutations in the gene encoding the P/Q Ca^{2+} channel α_{1A} subunit (*CACNA1A*) locate to the pore and voltage sensor regions and normally involve gain-of-channel function. We now report on a mutation identified in the first intracellular loop of CACNA1A ($\alpha_{1A(A454T)}$) that does not cause FHM but is associated with the absence of sensorimotor symptoms in a migraine with aura pedigree. $\alpha_{1A(A454T)}$ channels showed weakened regulation of voltage-dependent steady-state inactivation by $Ca_V\beta$ subunits. More interestingy, A454T mutation suppressed P/Q channel modulation by syntaxin 1A or SNAP-25 and decreased exocytosis. Our findings reveal the importance of I-II loop structural integrity in the functional interaction between P/Q channel and proteins of the vesicle-docking/fusion machinery, and that genetic variation in *CACNA1A* may be not only a cause but also a modifier of migraine phenotype.

CaV 2.1 (P/Q) channels | SNARE proteins | migraine with aura

Familial hemiplegic migraine (FHM) is an autosomal dominantly inherited subtype of migraine with aura that features some degree of hemiparesis during attacks (1, 2). The generally accepted view on migraine pathophysiology points to cortical spreading depression (CSD), an abnormal increase of cortical activity—followed by a long-lasting neuronal suppression wave—that propagates across the cortex, as the cause of the aura and migraine itself (1, 3). FHM-causing mutations have been reported in the *CACNA1A* gene (encoding the P/Q Ca^{2+} channel α_1 subunit) (4), resulting in a gain of P/Q channel function, mainly due to a reduction in the voltage threshold of channel activation favoring CSD initiation and propagation (1, 5–11). Other genetic and environmental factors may also play a role in shaping the phenotype, as identical mutations show different clinical characteristics (2).

The P/Q Ca^{2+} channel contains a pore-forming α_{1A} subunit and several regulatory subunits, including intracellular β subunits ($Ca_V\beta_{1-4}$) that bind to the intracellular loop between transmembrane domains I and II of α_{1A} (see Fig. 1*B* for an illustration of the channel complex). The effect of the regulatory subunits is essential for increasing the expression levels and modulating the voltage-dependent activation and inactivation of P/Q channels (12–15).

Presynaptic proteins of the vesicle-docking/fusion machinery, including plasma membrane SNARE proteins (syntaxin 1A and SNAP-25) and synaptotagmin, bind to a specific site (synprint) in the large intracellular loop connecting domains II and III of the P/Q channel α_{1A} subunit (Fig. 1*B*). This interaction allows secretory vesicles docking to the plasma membrane near the pathway for Ca^{2+} entry, optimizing neurotransmitter release. Syntaxin 1A and SNAP-25 also exert an inhibitory effect on P/Q channel activity by left-shifting the voltage dependence of steady-state inactivation (12, 16, 17). The synprint site serves an important anchoring function that may facilitate SNARE's modulation of channel gating, but the involvement of other still-unknown sites has been proposed (18). Disruption of voltage-gated Ca^{2+} channel-SNAREs interaction compromises vesicle exocytosis (19–22), as well as the inhibitory modulation of P/Q channels (23).

We next describe a CACNA1A mutation (A454T) that disturbs the functional interaction between SNAREs and the pore-forming α_{1A} subunit, resulting in mutant P/Q channels that are less efficiently coupled to secretion. This mutation, identified in a Spanish migraineur family, was not responsible for the disease but segregated with a different migraine phenotype lacking sensorimotor symptoms in their aura.

Results

Clinical and Genetic Spectrum of a Spanish Migraine Pedigree. Clinical analysis of the pedigree classified affected individuals as migraine with aura (MA) of the familial hemiplegic type (FHM), fulfilling all of the International Headache Society (IHS-II) criteria (II.3, II.5, III.2), nonhemiplegic MA displaying combinations of visual and sensory symptoms that include tongue and facial paresthesia (visual + sensory; II.6, III.1) and MA without sensorimotor—tongue/facial paresthesia or hemiplegia—symptoms (visual; I.2, II.1; Fig. 1*A*). Linkage analysis (and selected gene sequencing) of 11 polymorphic markers located within or flanking the four genes (*ATP1A2*, *SCN1A*, *SLC1A3*, and *CACNA1A*) previously involved in monogenic forms of migraine (1, 24) failed in the identification of the genetic cause of migraine in this pedigree (see Fig. S1*A* and *SI Methods* for details). However, we isolated a missense variation in exon 11 (c.1360G>A; Fig. S1*C*) of the *CACNA1A* gene (GenBank accession no. NM_001127221) in patients I.2 and II.1, which is not present in the rest of the probands nor in 300 chromosomes from unrelated Spanish nonmigraineurs. Genetic and clinical analysis suggested that 1360G>A mutation, resulting in an alanine-to-threonine

Author contributions: S.A.S., E.C.-L., A.L., M.A.V., A.M., B.C., and J.M.F.-F. designed research; S.A.S., E.C.-L., A.L., F.R.-M., C.P., and J.M.F.-F. performed research; S.A.S., F.R.-M., C.P., O.C., and N.F.-C. contributed new reagents/analytic tools; S.A.S., E.C.-L., A.L., R.C., and J.M.F.-F. analyzed data; and M.A.V., A.M., B.C., and J.M.F.-F. wrote the paper.

The authors declare no conflict of interest.

This article is a PNAS Direct Submission.

[1]To whom correspondence should be addressed. E-mail: jmanuel.fernandez@upf.edu.

This article contains supporting information online at www.pnas.org/cgi/content/full/0908359107/DCSupplemental.

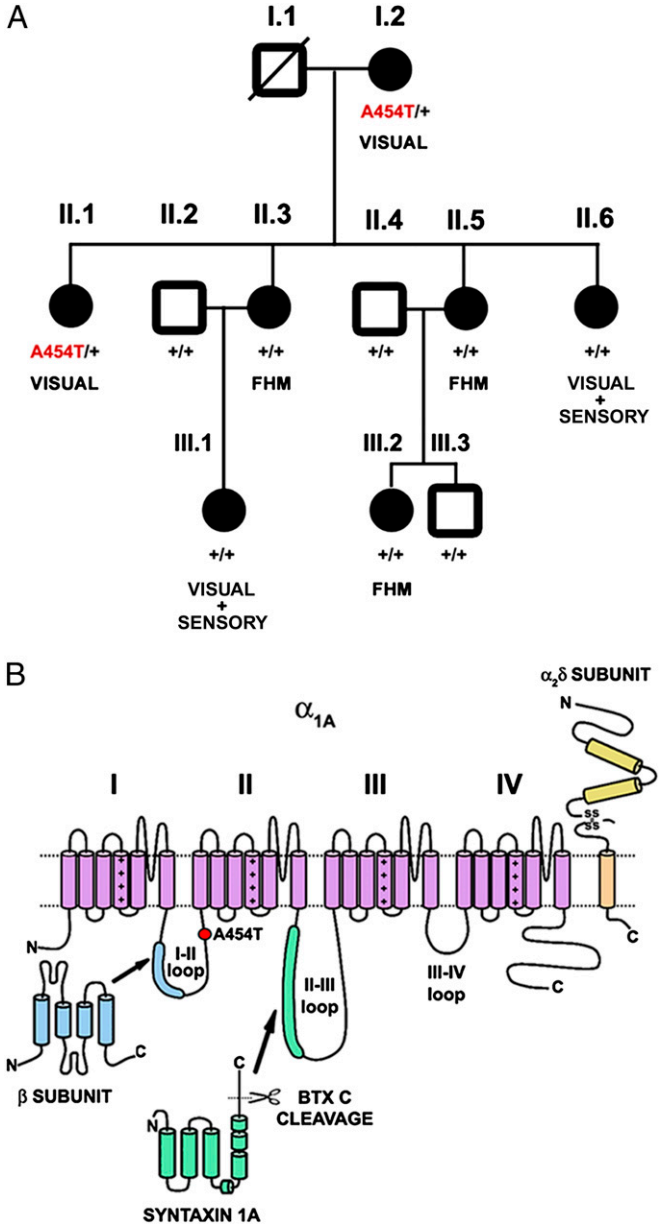

Fig. 1. Pedigree segregating the A454T mutation and protein location of the amino acid change. (*A*) Clinical and *CACNA1A* genetic characterization of a three-generation migraine with aura pedigree. Affected individuals are denoted by solid symbols (squares indicate male family members; circles, female family members; symbols with a slash, members who had died). The type of aura experienced is indicated below. (*B*) Location of the alanine-to-threonine mutation at position 454 (A454T) in the I-II intracellular loop of the P/Q channel α_{1A} subunit.

mutation at the highly conserved position 454 (A454T; Fig. 1*B* and Fig. S1*B*), was not the cause of migraine in the family under study. Instead, it appeared to modify the disease phenotype, because A454T carriers are the only migraineurs of the pedigree lacking tongue/facial paresthesic or hemiplegic symptoms. Therefore, we set up to analyze whether A454T *CACNA1A* mutation had any consequence on P/Q channel function.

Activation and Inactivation Properties of A454T Mutant P/Q Channels. Wild-type (WT) and mutant A454T α_{1A} ($\alpha_{1A(A454T)}$) rabbit subunits, together with accessory rat $Ca_V\beta$ and rabbit $\alpha_2\delta$ subunits, were expressed in HEK 293 cells and analyzed using the standard whole-cell patch-clamp technique. Mutation A454T had no effect on current density, activation parameters, deactivation and inactivation kinetics, and rate of recovery from inactivation of heterologously expressed P/Q channels (see Fig. S2 and *SI Methods* for details). The voltage dependence of inactivation was studied in WT and A454T P/Q channels. As expected (15), the voltage at which 50% of channels were inactivated ($V_{1/2,\ inact}$) shifted to more depolarized potentials for $Ca_V\beta_{2a}$-containing than for $Ca_V\beta_3$-containing WT P/Q channels (–3.05 ± 0.64 mV, n = 11 and –23.19 ± 0.45 mV, n = 10, respectively; $P < 0.001$) without changes in steepness (Fig. 2 *B*–*D*). A454T mutation produced a ~6 mV hyperpolarizing shift on $V_{1/2,\ inact}$ of channels containing $Ca_V\beta_{2a}$ (–9.23 ± 0.58 mV, n = 14; $P < 0.001$ vs. WT) and a ~6 mV depolarizing shift on $Ca_V\beta_3$-containing channels (–17.09 ± 0.55 mV, n = 9; $P < 0.001$ vs. WT). Differences between A454T channels containing $Ca_V\beta_{2a}$ or $Ca_V\beta_3$ subunits were still significant ($P < 0.001$). No changes were found in the slope factors for voltage-dependent inactivation between WT and A454T channels (Fig. 2*D*). These findings suggest that mutation A454T uncouples the effect of $Ca_V\beta$

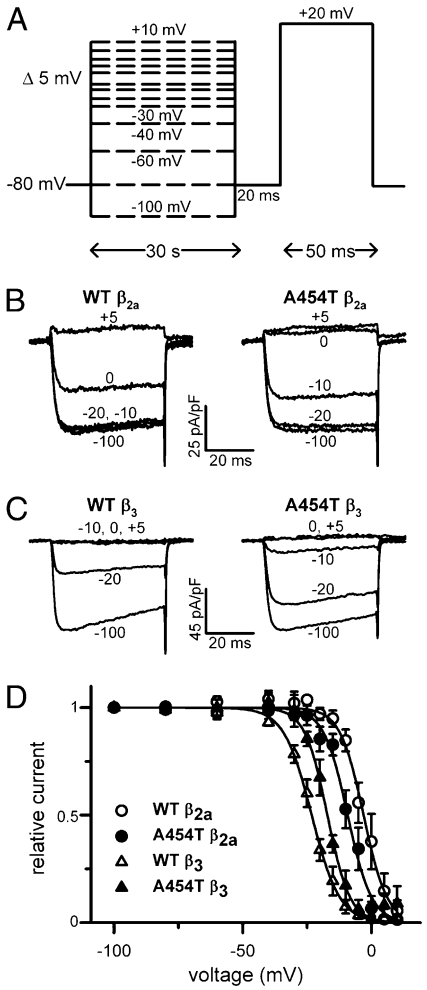

Fig. 2. A454T lessens modulation of P/Q channel activity by $Ca_V\beta$ subunits. Steady-state inactivation was studied with the voltage protocol shown (*A*). Typical traces obtained from cells expressing WT or A454T P/Q channels including either the β_{2a} (*B*) or the β_3 subunit (*C*). (*D*) Steady-state inactivation curves. WTβ_{2a} (○, n = 11); A454Tβ_{2a} (●, n = 14); WTβ_3 (△, n = 10), and A454Tβ_3 (▲, n = 9). Average k_{inact} for all four channel combinations were between –4.38 and –5.42 mV and did not differ statistically (ANOVA, P = 0.55).

PHYSIOLOGY

subunits on the voltage dependence of steady-state inactivation, placing the inactivation curves closer to the expected values for P/Q channels lacking regulatory $Ca_V\beta$s. We could not evaluate whether A454T affects $V_{1/2,\ inact}$ in the absence of $Ca_V\beta$s, because P/Q Ca^{2+} currents were negligible (Fig. S3).

A454T Affects Channel Regulation by Plasma Membrane SNAREs. Syntaxin 1A expression induced a significant ~10 mV left shift in the $V_{1/2,\ inact}$ of WT channels (Fig. 3 *A* and *B*; $P < 0.001$), whereas $V_{1/2,\ inact}$ was not altered by syntaxin 1A in A454T channels (Fig. 3 *A* and *C*; $P = 0.12$). Similarly, SNAP-25 promoted voltage-dependent inhibition of WT P/Q channels, as indicated by a significant ($P < 0.05$) decrease in the test pulse current following a prepulse to –20 mV, but had no effect on A454T P/Q channels (Fig. 3 *D* and *E*). Note that as A454T left-shifts the $Ca_V\beta_{2a}$-mediated steady-state inactivation, mutant channels showed higher inactivation than WT channels following a prepulse to –20 mV. Interestingly, the negative shift in the voltage-dependent steady-state inactivation induced by syntaxin 1A on WT P/Q channels was prevented by coexpression of the A454T but not WT I-II loop (Fig. 3 *F* and *G*). It is also worth noting the increased steady-state inactivation observed in the absence of syntaxin 1A regardless of the loop expressed (compared with the white bar of Fig. 3*E*), consistent with a functional uncoupling of $Ca_V\beta$ subunits due to binding competition with the I-II loops.

We also evaluated A454T P/Q channels in mouse pheochromocytoma cells (MPC 9/3L-AH) that present little or no endogenous voltage-gated Ca^{2+} current but contain vesicles and proteins involved in vesicle fusion, including syntaxin 1A and SNAP-25 (25). Electrophysiological properties of WT and A454T P/Q channels expressed in MPC 9/3L-AH cells were similar to those observed in HEK 293 cells in the presence of the $Ca_V\beta_3$ subunit, most probably due to preferred association of α_{1A} subunits with MPC endogenous $Ca_V\beta_3$ or β_1 rather than with expressed $Ca_V\beta_{2a}$ subunits (Fig. S4). Cleavage of syntaxin 1A by expressing botulinum toxin C (BTX C) (26) in MPC 9/3L-AH cells induced a significant increase in the test pulse current of WT P/Q channels following a prepulse to −20 mV (Fig. 4 *A* and *B*) or after stimulation with a train of short (2 ms) depolarizations at 200 Hz for 1.5 s (Fig. 4*C*). As previously reported by Zhong et al. (17) using this protocol, current remaining at the end of the train showed steady-state inactivation. In the case of MPC 9/3L-AH cells expressing WT P/Q channels, inactivation reached a 44.7 ± 5.5% ($n = 9$) or 17.8 ± 4.7% ($n = 5$) in the absence or presence of BTX C, respectively ($P < 0.01$). Expression of the neurotoxin had no significant effect on A454T channel inactivation; current remaining for A454T P/Q channels at the end of the train was inactivated by 17.9 ± 6.7% ($n = 6$) or 11.9 ± 3.6% ($n = 5$) in the absence or presence of BTX C, respectively (Fig. 4*C*). Cleavage of syntaxin 1A by BTX C was tested in HEK 293 cells overexpressing both proteins (Fig. 4*D*). These findings indicate that endogenous MPC syntaxin 1A can modulate the activity of heterologously expressed WT but not A454T P/Q channels, in agreement with the data obtained from HEK 293 cells (see Fig. 3).

A454T Reduces Exocytosis. MPC 9/3L-AH cells transiently transfected with rabbit α_{1AWT} or $\alpha_{1A(A454T)}$ showed similar P/Q currents (Fig. 5*A*) and Ca^{2+} charge density (calculated by integrating the area under the current traces and normalizing by cell size; Fig. 5*D*) following stimulation with a train of five depolarizations. Despite similar Ca^{2+} entry, MPC 9/3L-AH cells expressing A454T channels showed reduced exocytosis (evaluated by measuring membrane capacitance changes; Fig. 5*B* and *E*). The gaps in the capacitance recordings represent stimulation times. The induced changes in capacitance are indicative of vesicle fusion and catecholamine release, because depolarizing stimulus triggered amperometric events from MPC 9/3L-AH

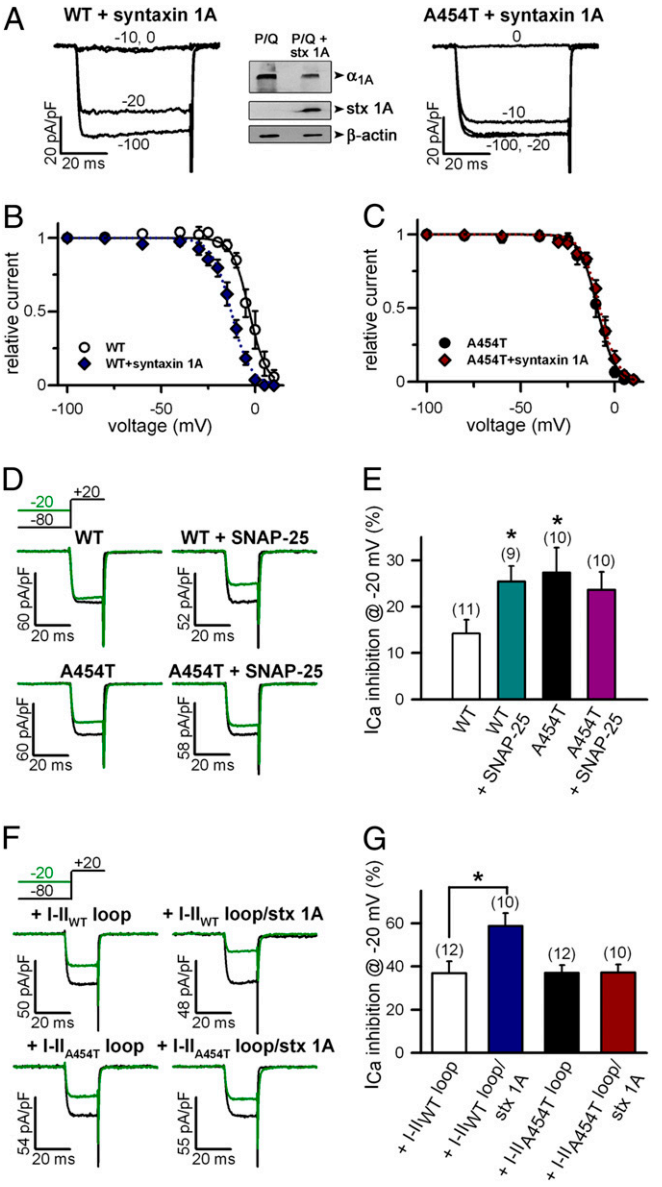

Fig. 3. A454T prevents modulation of P/Q channel activity by syntaxin 1A and SNAP-25. (*A*) Representative current traces from cells expressing WT (*Left*) or A454T (*Right*) P/Q channels in the presence of syntaxin 1A (to compare in the absence of syntaxin 1A see Fig. 2*B*). Western blot of plasma membrane proteins obtained from HEK 293 cells transfected with CFP-α_{1A}, $Ca_V\beta_{2a}$, and $\alpha_2\delta$ P/Q channel subunits in the absence or presence of syntaxin 1A and probed with anti-GFP, syntaxin 1A, and β-actin antibodies. Heterologous expression of P/Q channel subunits does not induce the expression of endogenous syntaxin 1A. Methodological details can be found in *SI Methods*. (*B* and *C*) Steady-state inactivation curves. $V_{1/2,inact}$ and k_{inact} values were (in mV): WT (○, $n = 11$) –3 ± 0.6 and –4.5 ± 0.5; WT + syntaxin 1A (◆, $n = 22$) –12.8 ± 0.5 and –5.1 ± 0.4; A454T (●, $n = 14$) –9.2 ± 0.5 and –4.6 ± 0.5; A454T + syntaxin 1A (◆, $n = 15$) –7.8 ± 0.5 and –4.8 ± 0.5. (*D*) Inhibition of WT and A454T P/Q channels alone (*Left*) or coexpressed with SNAP-25 (*Right*) evoked by a 20-ms test pulse to +20 mV following a 30-s prepulse to –80 mV (black trace) or –20 mV (green trace). (*E*) Average percentage I_{Ca} inhibition of WT and A454T P/Q channels in the absence or presence of SNAP-25. Ca^{2+} currents obtained as indicated in *D* were normalized to the current following the –80 mV prepulse. *$P < 0.05$ vs. WT. (*F*) Representative current traces from HEK 293 cells expressing WT P/Q channels coexpressed with WT (I-II_{WT} loop) or A454T (I-II_{A545T} loop) intracellular loops connecting domains I and II in the absence or presence of syntaxin 1A (stx 1A). Ca^{2+} currents were evoked by a 20-ms test pulse to +20 mV following a 30-s prepulse to –80 mV (black trace) or –20 mV (green trace). (*G*) Average percentage of WT P/Q I_{Ca} inhibition obtained under the experimental conditions shown in *F* (*$P < 0.01$).

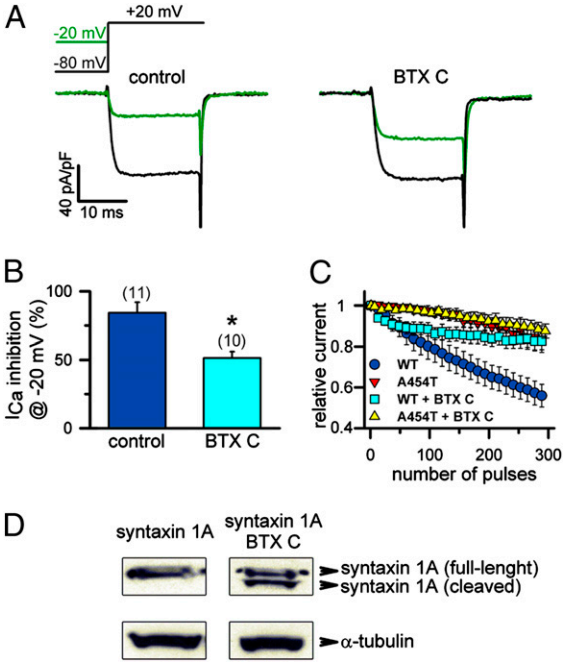

Fig. 4. Mutation A454T prevents P/Q channel regulation by MPC endogenous syntaxin 1A. (*A*) Inhibition of WT P/Q channels alone (*Left*, control) or coexpressed with BTX C (*Right*) in mouse pheochromocytoma (MPC 9/3L-AH) cells, evaluated as described in Fig. 3. (*B*) Average percentage I_{Ca} inhibition for WT P/Q channels expressed alone (control) or with BTX C in MPC 9/3L-AH cells. Ca^{2+} currents were normalized to the current following the −80-mV prepulse. $*P < 0.01$. (*C*) Average current evoked by every 10th pulse of a 200-Hz train of 2-ms depolarizations from −80 mV to +20 mV, normalized to the current evoked by the first pulse of the train, obtained from MPC 9/3L-AH cells expressing WT or A454T P/Q channels alone or coexpressed with BTX C, as indicated. (*D*) Western blot of cell lysates obtained from HEK 293 cells expressing syntaxin 1A alone or with botulinum toxin C (BTX C) and probed with anti-syntaxin 1A and α-tubulin antibodies. Full-length and cleaved syntaxin 1A are detected in the presence of BTX C. Methodological details can be found in *SI Methods*.

cells expressing P/Q channels loaded with dopamine (Fig. 5*C*). At intermediate intracellular calcium buffering (1 mM EGTA), expression of rabbit $\alpha_{1A(A454T)}$ subunit significantly reduced secretion efficiency, estimated by normalizing capacitance changes by Ca^{2+} charge density (as exocytosis is a steep function of Ca^{2+} influx). Such reduction was patent from the first depolarizing pulse, which mainly mobilized those vesicles located physically closer to release sites, i.e., vesicles defining the readily releasable pool (RRP), suggesting that A454T uncouples P/Q channels from secretory vesicles (Fig. 5*E*). Previous studies have shown that disruption of the interaction between voltage-gated calcium channels and SNARE proteins by a synprint peptide make less probable synaptic transmission by shifting its Ca^{2+} dependence to higher values (20). Therefore, we evaluated the effect of A454T on secretion efficiency under different calcium buffering conditions. This maneuver impacts the magnitude of cytoplasmic Ca^{2+} domains and modifies the amount of vesicles capable of sensing such Ca^{2+} signals, depending on its proximity to the calcium entry pathway (20, 27). As expected, secretion efficiency was inversely proportional to EGTA concentration (Fig. 5*E*). Addition of an excess of exogenous calcium buffer (5 mM EGTA) to the cytoplasm, which restricts calcium signals, reduced the secretion evoked by a train of stimuli in both α_{1AWT}- and $\alpha_{1A(A454T)}$-expressing cells (Fig. 5*E*), whereas a decrease in cytosolic EGTA (0.1 mM) rescued the effect of the A454T mutation on exocytosis (Fig. 5*E*).

Finally, a similar decrease in the efficiency of P/Q channel coupling to exocytosis at intermediate intracellular calcium buffering (1 mM EGTA) was observed when introducing the A454T mutation in the human α_{1A} subunit (Fig. 5 *F* and *G* and Fig. S5).

Discussion

The A454T mutation was initially considered a polymorphic variant with a frequency of 0.02 (4), and more recently has been associated to early onset progressive ataxia (28). However, none of the two A454T carriers included in our study presented cerebellar symptoms despite their advanced ages (72 and 49 years). A454T does not cosegregate with migraine in our pedigree, but the two A454T migraineurs display a milder migraine phenotype with visual aura only and no sensorimotor symptoms. This clinical observation, together with the fact that the mutation was not present in 300 control chromosomes and involved a highly conserved amino acid within an important regulatory domain of the channel (the I-II intracellular loop of CACNA1A) prompted us to evaluate the impact of the A454T mutation on P/Q channel activity.

A454T P/Q channel presents a disrupted regulation of the voltage dependence of steady-state channel inactivation by auxiliary $Ca_V\beta$ subunits. Voltage-dependent inactivation of Ca^{2+} channels is an important physiological mechanism that contributes to the short-term depression of neurosecretion (29, 30), but its contribution to migraine pathophysiology remains to be solved (5–8, 10, 11). Current density, inactivation kinetics, and voltage dependence of channel activation remained unaltered, suggesting that the effect of A454T mutation on steady-state channel inactivation is not due to the removal of $Ca_V\beta$ binding to the α_{1A} subunit (also supported by the fact that overexpression of either WT or A454T I-II loops antagonized the effect of $Ca_V\beta_{2a}$ on channel activity). Instead, it may be explained by a structural alteration of the I-II loop due to the A454T mutation that affects the intramolecular transduction by which $Ca_V\beta$-α_{1A} interaction modulates channel inactivation. Although it has been suggested that alterations in the kinetics and voltage dependence of steady-state inactivation are linked (31), a report examining FHM-causing *CACNA1A* mutations has already shown that both parameters change independently (8).

Our data also suggests that A454T impairs the interaction between plasma membrane SNARE proteins (syntaxin 1A and SNAP-25) and P/Q channels. This is based on (*i*) loss of SNARE-dependent modulation of channel steady-state inactivation, (*ii*) removal of P/Q channel regulation by syntaxin 1A following expression *in trans* of the A454T but not WT I-II loop, and (*iii*) reduction in secretion efficiency of A454T P/Q channel.

Docking of the vesicle-releasing machinery to the source of Ca^{2+} in the presynaptic membrane is critical for the high efficiency of neurotransmitter release. SNARE proteins have a key role in this process by positioning docked vesicles near calcium entry channels (19–22) and by recruiting synaptic vesicles to presynaptic Ca^{2+} channel clusters during repetitive or long-lasting depolarizations (32). Although the molecular mechanisms underlying these processes are not unequivocally demonstrated, it has been postulated that SNARE proteins participate via their binding to the channel α_1 subunit (12, 18). Accordingly, impairment of the SNARE proteins interaction with calcium channels reduces the efficiency of synaptic transmission (19–22). A454T induces a ~49% reduction in secretion following a depolarizing train, although a significant ~44% decrease was already detected from the first pulse, thereby supporting the view that A454T-expressing cells present mislocalization of synaptic vesicles near Ca^{2+} channels. The magnitude of the fall in exocytosis induced by the A454T mutation is very close to that reported for a partial deletion of the synprint site that interferes in the interaction between SNAREs and voltage-gated N-type Ca^{2+} channel expressed in MPC 9/3L-AH cells (21). The mere removal of the inhibitory action of SNAREs on channel gating by the A454T

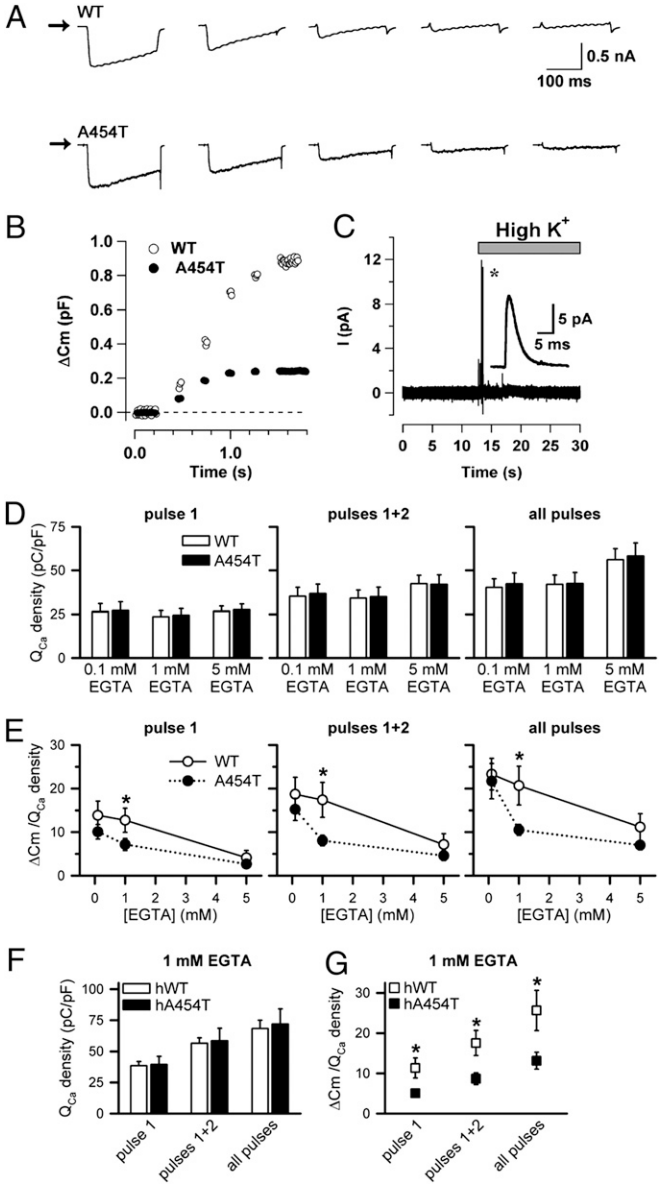

Fig. 5. Mutation A454T decreases secretion efficiency. (*A*) Currents from two MPC 9/3L-AH cells expressing either WT (*Upper*) or A454T channels (*Lower*) in response to a train of five successive 200-ms depolarizing voltage steps to +20 mV delivered at 20 Hz. Arrows indicate the 0 current level. (*B*) Capacitance traces, plotted as a function of time, from the same cells showed in *A*. WT (○) and A454T (●) P/Q-expressing cells were stimulated at 20 Hz as described. (*C*) Amperometric recording from a MPC 9/3L-AH cell loaded with dopamine during the application of a local puff of a depolarizing high-K^+ solution. Note the synchronous release of dopamine after the onset of the stimulus. (*Inset*) Higher time-scale resolution of the amperometric spike indicated with an asterisk. (*D*) Averaged data for Ca^{2+} influx normalized by the whole-cell capacitance [Q_{Ca} density (pC/pF)] elicited by the first depolarizing pulse, the first two depolarizing pulses, and all five depolarizing pulses (as indicated) under three different intracellular Ca^{2+}-buffering conditions in WT (EGTA 0.1 mM, $n = 8$; EGTA 1 mM, $n = 21$; EGTA 5 mM, $n = 7$) and A454T MPC 9/3L-AH transfected cells (EGTA 0.1 mM, $n = 10$; EGTA 1 mM, $n = 21$; EGTA 5 mM, $n = 7$). (*E*) Exocytosis [ΔCm (fF)] normalized as a function of Ca^{2+} entry [Q_{Ca} density (pC/pF)] corresponding to the conditions described in *D*. $*P < 0.05$. (*F*) Averaged data for Ca^{2+} influx normalized by cell size [Q_{Ca} density (pC/pF)] elicited by the first depolarizing pulse, the first two depolarizing pulses, and all five depolarizing pulses (as indicated) under intermediate intracellular Ca^{2+}-buffering conditions (1 mM EGTA) in MPC 9/3L-AH cells transfected with either the human WT (hWT, $n = 12$) or human A454T (hA454T, $n = 7$) P/Q channel. (*G*) Exocytosis [ΔCm (fF)] normalized as a function of Ca^{2+} entry [Q_{Ca} density (pC/pF)] corresponding to the conditions described in *F*. $*P < 0.05$.

mutation would not explain the reduced vesicle secretion (22). Also supporting the vesicle mislocalization hypothesis with A454T channels is our observation that the secretory response of $\alpha_{1A(A454T)}$-expressing cells is rescued when the intracellular concentration of EGTA is lowered, which increases Ca^{2+} diffusion and promotes the release of vesicles away from the Ca^{2+} entry pathway. Efficient secretion with A454T P/Q channels is shifted to higher Ca^{2+} levels, an effect also reported for the action of a synprint peptide on synaptic release through the uncoupling of N-type calcium channels and SNARE proteins (20). However, the fact that the secretory response of cells expressing mutant A454T P/Q channels show lower sensitivity when increasing EGTA from 1 mM to 5 mM is inconsistent with the interpretation that the mutation disrupts the localization of synaptic vesicles near Ca^{2+} channels. For this interpretation to be adequate we should expect a larger relative reduction of secretion in $\alpha_{1A(A454T)}$-expressing cells when increasing EGTA concentration to 5 mM, because an excess of calcium buffer impairs the buildup of intracellular Ca^{2+} domains and will mainly reduce the fusion of those vesicles not linked to Ca^{2+} channels. Therefore, we cannot discard the possibility that the mutation somehow would alter the sensitivity of the calcium sensor in the exocytotic machinery, without affecting vesicle localization. Moreover, as the negative effect of A454T mutation on exocytosis depends on cytosolic Ca^{2+}-buffering conditions, its impact might vary at different synapses because presynaptic calcium microdomains can be modified by the particular endogenous calcium buffers (33), which differ from neuron to neuron.

The mechanisms underlying the effects of A454T could be explained by a modification in the structure of the I-II loop. This may spoil the three-dimensional arrangement of *CACNA1A* intracellular domains, which, in turn, alters the interaction pattern between α_{1A} cytoplasmic domains (34). This is a unique description of a naturally occurring mutation that affects one of the most important specializations of the P/Q Ca^{2+} channel: the modulation of exocytosis in concert with presynaptic SNARE proteins (22, 32). Our data highlights the importance of I-II loop structural integrity in the functional interaction of P/Q channel with proteins of the SNARE complex to maintain an optimal synaptic transmission. This observation agrees with recent reports that view cross-talks between cytosolic regions of α_{1A} as important processes in channel function (14, 34), and supports the idea that regulation of voltage-gated Ca^{2+} channels by SNARE proteins require the integrity of channel domains additional to the synprint (18).

In conclusion, three main points relevant to the molecular physiology and pathology of P/Q channel can be drawn from our study: (*i*) A454T-induced misregulation involves changes in voltage dependence of steady-state inactivation. The functional relevance of these changes builds up during and after high-frequency neuronal firing, such as those occurring during CSD in migraine patients (1, 35), although by now it is difficult to establish a correlation between these changes and the observed clinical phenotype in A454T carriers. (*ii*) The impairment of functional interaction between syntaxin 1A/SNAP-25 and A454T P/Q channels highlights the relevance of the I-II loop as an integrator of channel regulatory mechanisms that also include SNARE proteins. The negative effect of the mutation on P/Q channel coupling to secretion might result in decreased CSD propagation. This may be particularly relevant in sensorimotor cortical areas where CSD triggering is more reluctant than in the occipital visual area (36), thus explaining the absence of sensorimotor aura in A454T carriers. Furthermore, because *CACNA1A* genetic variations associated to ataxia involve loss of channel function (37), the reduced secretion efficiency of A454T P/Q channels may lie beneath the development of cerebellar symptoms in some patients (28). (*iii*) Finding how this mutation integrates into the physiology of native P/Q channel expressing neurons, as well as the confirmation of the putative effect of A454T preventing sensorimotor auras in larger migraine pedi-

grees, is essential to consider *CACNA1A* not only a disease-causing but a modifier gene as well.

Methods

DNA Constructs and Site-Directed Mutagenesis. Rabbit α_{1A} ($Ca_V2.1$) and $\alpha_2\delta$; rat $Ca_V\beta_{2a}$, $Ca_V\beta_3$, and syntaxin 1A were all subcloned into pcDNA3 expression vector. Rabbit WT α_{1A} was also subcloned into pcDNA3-NCFP vector, 3′ from the fluorescent tag, between 5′ BamHI and 3′ XhoI restriction enzyme sites. Human SNAP-25 was cloned into pEGFP-C3 and botulinum toxin C (BTX C) into pIRES expression vector. The A454T mutation was introduced into rabbit α_{1A} cDNA using the QuikChange Site-Directed Mutagenesis XL kit (Stratagene), forward (5′-GGGGTCTCCCTTTACCCGAGCCAGCATTAA-3′) and a reverse (5′-TTAATGCTGGCTCGGGTAAAGGGAGACCCC-3′) primers. *CACNA1A* I-II intracellular loop was amplified by PCR (forward primer 5′-CGGAATTCGCCAC-CATGGGGGAGTTTGCCAAAGAAAG-3′ and reverse primer 5′-CCGCTCGAGC-TAGGCCTGAGTTTTGACCATG-3′) from rabbit WT and A454T pcDNA3-α_{1A} and cloned into pcDNA3 using 5′ EcoRI and 3′ XhoI restriction sites. Human α_{1A} was originally cloned into pCMV vector, and mutation A454T was introduced by site-directed mutagenesis (GenScript Corp.). All cDNA clones used in this study were sequenced in full to confirm their integrity.

Heterologous Expression, Electrophysiology, Capacitance, and Amperometric Measurements. HEK 293 cells were transfected using polyethylenimine ExGen500 (Fermentas Inc.) per the manufacturer's instructions. Rabbit α_{1AWT} or $\alpha_{1A(A454T)}$ constructs were coexpressed with rat $Ca_V\beta$ subunits (β_{2a} or β_3), rabbit $\alpha_2\delta$, and EGFP as a transfection marker, using the ratio for α_{1A}, $Ca_V\beta$, $\alpha_2\delta$, and EGFP of 1:1:1:0.3. In some experiments, syntaxin 1A, SNAP-25, I-II $_{WT}$ loop, I-II $_{A454T}$ loop, and/or BTX C were also transfected at least at the same ratio as P/Q channel subunit cDNAs. MPC cell line 9/3L-AH was transfected using Lipofectamine Plus (Invitrogen) at the same constructs ratio applied for HEK 293 patch-clamp experiments. Recordings were done 48–72 h after transfection.

Whole-cell P/Q calcium currents (I_{Ca}) were measured using pipettes (2-3 MΩ) filled with a solution containing (in mM): 13 CsCl, 120 caesium acetate, 2.5 $MgCl_2$, 10 Hepes, 1 EGTA, 4 Na_2ATP, and 0.1 Na_3GTP (pH 7.2–7.3 and 295–300 mosmoles/l). The external solution contained (in mM): 140 NaCl, 3 KCl, 2.5 $CaCl_2$, 1.2 $MgCl_2$, 10 Hepes, and 10 glucose (pH 7.3–7.4 and 300–305 mosmoles/l) for HEK 293 cells, and 140 tetraethylammonium-Cl, 5 $CaCl_2$, 10 Hepes, and 10 glucose (pH 7.3; 300 mosmol/L) for MPC 9/3L-AH cells. Full details about electrophysiology protocols are provided in *SI Methods*.

Capacitance measurements were performed using an EPC-9 patch-clamp amplifier (HEKA Electronics, Lambrecht/Pfalz, Germany) using the "sine + dc" software lock-in amplifier method implemented in PULSE software. Further details are provided in *SI Methods*.

Amperometric recordings were carried out on MPC 9/3L-AH cells loaded with dopamine triggered to secrete by local puffing of a high-K^+ extracellular solution. Further details are provided in *SI Methods*.

All experiments were carried out at room temperature (22–24 °C).

Statistics. Data are presented as the means ± SEM. Statistical tests included Student's *t* test, ANOVA, followed by a Bonferroni post hoc test or non-parametric ANOVA (Kruskal–Wallis test), followed by a Dunn post hoc test, as appropriate. Differences were considered significant if $P < 0.05$.

ACKNOWLEDGMENTS. We thank Dr. Birnbaumer (National Institutes of Health) for providing P/Q channel cDNAs, Dr. Blasi (Universitat de Barcelona) for providing syntaxin 1A and botulinum toxin C cDNAs, Dr. Criado (Universidad Miguel Hernández) for providing SNAP-25 cDNA, Dr. J. Striessnig (University of Innsbruck) for the gift of human CACNA1A cDNA, and Dr. Harkins for making available the MPC cell line 9/3L-AH. Dr. Marfany and Dr. Fandos are acknowledged for helpful suggestions on the DNA cloning experiments. We thank Dr. Fernandes for her help in preliminary electrophysiological studies and M. Elías for assistance in the amperometric recordings. The work was funded by Fundació la Marató de TV3 (061331 and 061330), the Spanish Ministry of Education and Science (SAF2006-13893-C02-02, SAF2006-13893-C02-01, SAF2009-13182-C03-02, SAF2009-13182-C03-01, SAF2009-13182-C03-03, SAF2003-04704, SAF2006-04973, and SAF2009-09848), Fondo de Investigación Sanitaria (red HERACLES RD06/0009, Red Española de Ataxias G03/056, PI05/2129, and PI05/1050), and Generalitat de Catalunya (SGR05-848, SGR05-266, 2009SGR1369, 2009SGR971 and 2009SGR78). M.A.V. is the recipient of an ICREA Academia Award (Generalitat de Catalunya).

1. Pietrobon D (2007) Familial hemiplegic migraine. *Neurotherapeutics* 4:274–284.
2. Ducros A, et al. (2001) The clinical spectrum of familial hemiplegic migraine associated with mutations in a neuronal calcium channel. *N Engl J Med* 345:17–24.
3. Bolay H, et al. (2002) Intrinsic brain activity triggers trigeminal meningeal afferents in a migraine model. *Nat Med* 8:136–142.
4. Ophoff RA, et al. (1996) Familial hemiplegic migraine and episodic ataxia type-2 are caused by mutations in the Ca^{2+} channel gene CACNL1A4. *Cell* 87:543–552.
5. Kraus RL, Sinnegger MJ, Glossmann H, Hering S, Striessnig J (1998) Familial hemiplegic migraine mutations change α_{1A} Ca^{2+} channel kinetics. *J Biol Chem* 273:5586–5590.
6. Hans M, et al. (1999) Functional consequences of mutations in the human α_{1A} calcium channel subunit linked to familial hemiplegic migraine. *J Neurosci* 19:1610–1619.
7. Kraus RL, et al. (2000) Three new familial hemiplegic migraine mutants affect P/Q-type $Ca^{(2+)}$ channel kinetics. *J Biol Chem* 275:9239–9243.
8. Müllner C, Broos LA, van den Maagdenberg AM, Striessnig J (2004) Familial hemiplegic migraine type 1 mutations K1336E, W1684R, and V1696I alter $Ca_v2.1$ Ca^{2+} channel gating: Evidence for β-subunit isoform-specific effects. *J Biol Chem* 279:51844–51850.
9. van den Maagdenberg AM, et al. (2004) A *Cacna1a* knockin migraine mouse model with increased susceptibility to cortical spreading depression. *Neuron* 41:701–710.
10. Tottene A, et al. (2005) Specific kinetic alterations of human $Ca_V2.1$ calcium channels produced by mutation S218L causing familial hemiplegic migraine and delayed cerebral edema and coma after minor head trauma. *J Biol Chem* 280:17678–17686.
11. Serra SA, et al. (2009) The hemiplegic migraine-associated Y1245C mutation in CACNA1A results in a gain of channel function due to its effect on the voltage sensor and G-protein-mediated inhibition. *Pflugers Arch* 458:489–502.
12. Catterall WA (2000) Structure and regulation of voltage-gated Ca^{2+} channels. *Annu Rev Cell Dev Biol* 16:521–555.
13. Jones SW (2002) Calcium channels: When is a subunit not a subunit? *J Physiol* 545:334.
14. Stotz SC, Jarvis SE, Zamponi GW (2004) Functional roles of cytoplasmic loops and pore lining transmembrane helices in the voltage-dependent inactivation of HVA calcium channels. *J Physiol* 554:263–273.
15. Birnbaumer L, et al. (1998) Structures and functions of calcium channel β subunits. *J Bioenerg Biomembr* 30:357–375.
16. Bezprozvanny I, Scheller RH, Tsien RW (1995) Functional impact of syntaxin on gating of N-type and Q-type calcium channels. *Nature* 378:623–626.
17. Zhong H, Yokoyama CT, Scheuer T, Catterall WA (1999) Reciprocal regulation of P/Q-type Ca^{2+} channels by SNAP-25, syntaxin and synaptotagmin. *Nat Neurosci* 2:939–941.
18. Bezprozvanny I, Zhong P, Scheller RH, Tsien RW (2000) Molecular determinants of the functional interaction between syntaxin and N-type Ca^{2+} channel gating. *Proc Natl Acad Sci USA* 97:13943–13948.
19. Mochida S, Sheng Z-H, Baker C, Kobayashi H, Catterall WA (1996) Inhibition of neurotransmission by peptides containing the synaptic protein interaction site of N-type Ca^{2+} channels. *Neuron* 17:781–788.
20. Rettig J, et al. (1997) Alteration of Ca^{2+} dependence of neurotransmitter release by disruption of Ca^{2+} channel/syntaxin interaction. *J Neurosci* 17:6647–6656.
21. Harkins AB, Cahill AL, Powers JF, Tischler AS, Fox AP (2004) Deletion of the synaptic protein interaction site of the N-type ($Ca_V2.2$) calcium channel inhibits secretion in mouse pheochromocytoma cells. *Proc Natl Acad Sci USA* 101:15219–15224.
22. Keith RK, Poage RE, Yokoyama CT, Catterall WA, Meriney SD (2007) Bidirectional modulation of transmitter release by calcium channel/syntaxin interactions *in vivo*. *J Neurosci* 27:265–269.
23. Bergsman JB, Tsien RW (2000) Syntaxin modulation of calcium channels in cortical synaptosomes as revealed by botulinum toxin C1. *J Neurosci* 20:4368–4378.
24. Jen JC, Wan J, Palos TP, Howard BD, Baloh RW (2005) Mutation in the glutamate transporter EAAT1 causes episodic ataxia, hemiplegia, and seizures. *Neurology* 65:529–534.
25. Harkins AB, Cahill AL, Powers JF, Tischler AS, Fox AP (2003) Expression of recombinant calcium channels support secretion in a mouse pheochromocytoma cell line. *J Neurophysiol* 90:2325–2333.
26. Schiavo G, Shone CC, Bennett MK, Scheller RH, Montecucco C (1995) Botulinum neurotoxin type C cleaves a single Lys-Ala bond within the carboxyl-terminal region of syntaxins. *J Biol Chem* 270:10566–10570.
27. Moser T, Neher E (1997) Rapid exocytosis in single chromaffin cells recorded from mouse adrenal slices. *J Neurosci* 17:2314–2323.
28. Cricchi F, et al. (2007) Early-onset progressive ataxia associated with the first *CACNA1A* mutation identified within the I-II loop. *J Neurol Sci* 254:69–71.
29. Branchaw JL, Banks MI, Jackson MB (1997) Ca^{2+}- and voltage-dependent inactivation of Ca^{2+} channels in nerve terminals of the neurohypophysis. *J Neurosci* 17:5772–5781.
30. Forsythe ID, Tsujimoto T, Barnes-Davies M, Cuttle MF, Takahashi T (1998) Inactivation of presynaptic calcium current contributes to synaptic depression at a fast central synapse. *Neuron* 20:797–807.
31. Sandoz G, et al. (2004) Repositioning of charged I-II loop amino acid residues within the electric field by β subunit as a novel working hypothesis for the control of fast P/Q calcium channel inactivation. *Eur J Neurosci* 19:1759–1772.
32. Wadel K, Neher E, Sakaba T (2007) The coupling between synaptic vesicles and Ca^{2+} channels determines fast neurotransmitter release. *Neuron* 53:563–575.
33. Neher E, Sakaba T (2008) Multiple roles of calcium ions in the regulation of neurotransmitter release. *Neuron* 59:861–872.
34. Geib S, et al. (2002) The interaction between the I-II loop and the III-IV loop of $Ca_v2.1$ contributes to voltage-dependent inactivation in a β-dependent manner. *J Biol Chem* 277:10003–10013.
35. Black DF (2006) Sporadic and familial hemiplegic migraine: Diagnosis and treatment. *Semin Neurol* 26:208–216.
36. Lauritzen M (1994) Pathophysiology of the migraine aura. The spreading depression theory. *Brain* 117:199–210.
37. Ducros A, Tournier-Lasserve E, Bousser MG (2002) The genetics of migraine. *Lancet Neurol* 1:285–293.